UCRL- 92426
PREPRINT

THE TRANSPORT OF 14 MeV NEUTRONS THROUGH HEAVY MATERIALS 150 < A < 208

L. F. Hansen, H. M. Blann, R. J. Howerton,
T. T. Komoto, and B. A. Pohl

Lawrence Livermore National Laboratory
University of California
Livermore, CA 94550

This paper was prepared for submittal to
Nuclear Science and Engineering

April 1985

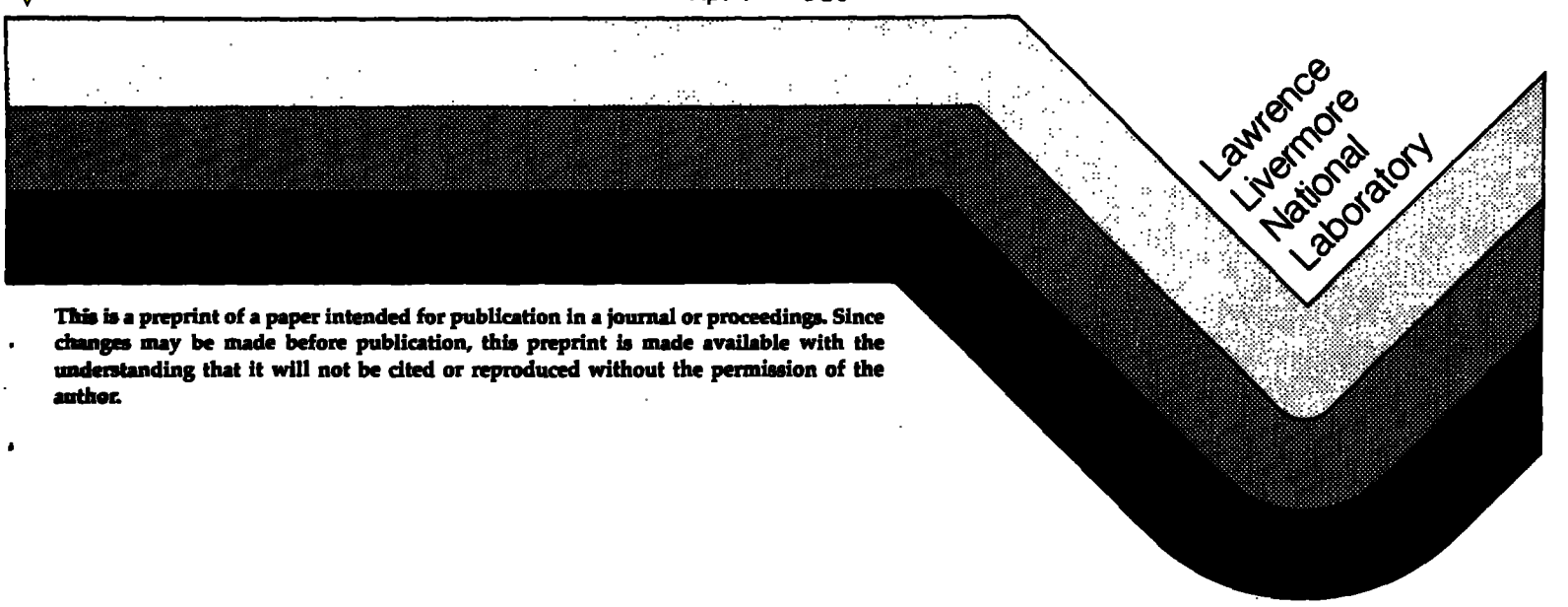

The Transport of 14 MeV Neutrons Through Heavy Materials

$150 < A < 208$*

L. F. Hansen, H. M. Blann, R. J. Howerton, T. T. Komoto,

and B. Pohl

Lawrence Livermore National Laboratory

University of California

Livermore, CA 94550

ABSTRACT

The emission spectra from Holmium (0.8 mean free path, mfp), Tantalum (1 and 3 mfp), Gold (1.9 mfp) and Lead (1.0 mfp) have been measured using the sphere transmission and time-of-flight (TOF) techniques. The 14 MeV incident neutrons are from the Livermore Insulated-Core-Transformer (ICT) accelerator using the $^{3}H(d,n)^{4}He$ reaction. These materials were chosen to span a wide range of heavy nuclei, including deformed (Ho and Ta), spherical (Au) and closed shell (Pb) nuclei. The neutron emission spectra have been measured in the energy interval of 1 to 15 MeV and the results compared with Monte Carlo calculations performed using the neutron-photon transport code TART and evaluated neutron cross sections files. An alternative representation of the secondary neutron spectra has been carried out by using model calculations for precompound processes and collective effects in the calculations of the pulsed sphere emission spectra. Their importance in the quality of the agreement between measurements and calculations is discussed. The measurements are compared with the predictions of two evaluated neutron libraries, the ENDF/B-V and ENDL. In addition, calculations have been carried out using neutron cross sections calculated directly from well accepted nuclear models by the code ALICE/LIVERMORE 82 and by ECIS 79. The quality of the agreements between the measurements and calculations obtained with the latter cross sections and those from the ENDL library, are reasonably good for all the targets, and these are systematically better than the results obtained with the ENDF/B-V files. Discrepancies between measurements and calculations as large as 80% are found using the ENDF/B-V files for the emission of neutrons from gold in the 5-10 MeV energy range.

I. INTRODUCTION

The measurements presented in this paper have been carried out under the Pulsed Sphere Program[1-3] at Lawrence Livermore National Laboratory (LLNL). The objective of this program, which covers a span of more than ten years, has been to test the accuracy of codes, cross sections and physical assumptions used in the neutronic calculations of blanket design for fusion reactors and also for defense applications. This is accomplished by comparing calculations against measurements of the neutron emission spectra from materials of interest when bombarded with 14 MeV neutrons. Spherical geometry, single materials, or simple compounds used in these measurements facilitate the interpretation of the results when discrepancies between measurements and calculations are found.

The present materials were chosen to cover a wide range of heavy nuclei characterized by different nuclear structure as a result of their shape and closure of neutron and proton shells. These features in turn, influence the energy distribution of the secondary neutrons as will be shown later. Holmium and tantalum are strongly deformed nuclei, while gold and lead are spherical nuclei. In addition, in lead both neutron and proton shells are closed for the isotope of greatest abundance. The interest in these materials results from their use in shielding applications and in defense applications. Lead is of special interest since it has been proposed[4] as a neutron multiplier in some conceptual designs of fusion blankets. In all the above applications, these materials would be inmersed in a 14 MeV neutron flux which is modified by their presence. Consequently, it is important to be able to calculate the neutron and gamma leakage spectra accurately.

We have measured the neutron leakage spectra in the energy region of 1 to

15 MeV for the above materials using the sphere transmission and TOF techniques.[1] The radii of the spherical assemblies varies between 1 and 3 mfp for 14 Mev neutrons. Details of the measurements are given in Sec. II. The results have been compared with the predictions of Monte Carlo calculations using the ENDF/B-V and ENDL neutron cross sections libraries[5,6] which are used by the fusion community. The ENDL is the LLNL in-house library. For the nuclei under discussion, the ENDL/B-V library contains independent evaluations only for gold and lead. This library does not have an evaluation for holmium and the one for tantalum is from an earlier ENDL evaluation which presently has been superseded[7]. The calculations for gold with the ENDF/B-V library underpredict greatly the emission of neutrons with energies between 10 and 5 MeV. The absence of these high energy neutrons results from the omission of precompound processes in the reaction mechanisms accounting for the neutron production. The precompound mechanism is responsible for the presence of forward peaked high energy neutrons in the emission spectrum of the secondary neutrons.

The above deficiency found in the representation of the neutron emission spectra from materials bombarded with 14 MeV neutrons, was a common problem[8,9] for all the evaluations carried out with the ENDF/B-III library for medium and heavy nuclei (A > 24). Subsequent versions of ENDF (IV and V) have attempted to account for the presence of high energy neutrons in the measured spectra in two ways:

1) By including the contribution from the direct-interaction component in the calculations of the inelastic scattering. For example in Fe, this contribution has been included in 15 of the 26 levels that describe the (n,n') cross sections up to 4.53 MeV excitation energy.

2) By including a direct-interaction component in the continuum. This is

done using an empirical treatment[10] that allows a fit to the data. A similar approach has been followed in the ENDL library where, in contrast with the ENDL/B-V, only a couple of low excited levels or none, are included in the evaluations. The high energy inelastic neutrons (E > 5 MeV) are represented in ENDL by a differential energy spectrum that was derived empirically from the systematics of measured differential data.

Steps 1 and 2 have resulted in a marked improvement[2] in the agreement found between calculations carried out with the ENDF/B-V and integral measurements of the type described in this paper. Undoubtedly, the gold evaluation needs to be revised for the next edition of this library. The same type of improvement is observed in the fits obtained with the ENDL library. These calculations are discussed in Sec. III.

In addition to the two evaluated neutron libraries (ENDF/B-V and ENDL) used in the Monte Carlo calculations, a test library based on ENDL was generated in which the code[11] ALICE/LIVERMORE 82 was used. This code provided substitute differential data for reaction cross sections and spectra for (n,n') continium, (n,2n), (n,3n), (n,p), (n,n'p + n,pn'), (n,α) and (n,n'α + n,α,n') reactions for incident neutron energies from 2.0 to 20.0 MeV. A second test library was generated in which the elastic differential cross sections obtained from a coupled-channel calculation using deformed optical model potentials replaced the ENDL values used in the first test library (in both evaluated libraries, ENDL and ENDF/B-V, the elastic scattering cross sections were generated using optical model potentials for spherical nuclei). The coupled-channel calculation was carried out with the code[12] ECIS 79 and includes, in addition to the ground state (GS), the low lying excited levels belonging to the rotational band (Ho, Ta) or to the vibrational band (Au, Pb) built on the (GS) level. The excitation functions

and angular distributions of these collective levels in the 2.0 to 20.0 energy range were also included in the second test library. In the test libraries the precompound neutron emission is calculated using the geometry dependent hybrid (GDH) model[13,14]. The GDH model has been used in the present calculations because it is expected to give a better description of the nuclear interaction, i.e., a higher probability of surface interactions to undergo precompound decay than for central collisions.

The results of the calculations carried out with the evaluated and test libraries are discussed in Sec. III. Neither of the test libraries should be construed as "new evaluations" for these materials. The main objective in generating these "test libraries" has been to study whether or not microscopic cross section generated using coupled channel and pre-equilibrium models, can provide a better description of the pulsed sphere data.

II. EXPERIMENTAL APPARATUS AND PROCEDURE

The measurements of the neutron emission spectra have been made using spherical assemblies pulsed with a 14 MeV neutron source positioned at the center of the spheres. The 14 MeV nominal energy neutrons from the $T(d,n)^4He$ reaction are generated using the 400-keV D+ beam from the Livermore insulated-core-transformer (ICT) accelerator. The beam, swept at a 0.5 MHz rate and bunched to < 2 ns burst width, strikes a tritium-loaded titanium target mounted at the end of a low mass conical assembly, which positions the target at the center of the spherical assembly. The titanium, which absorbs the tritium, is 1.59 cm in diameter and 4 mg/cm^2 thick, and is evaporated on a 0.076 cm thick tungsten backing. Details on the geometry and composition of the low mass assembly can be found in Ref. 1. The 14 MeV neutron production at the tritium target is monitored by counting the associated alpha particle with a thin (25 um) silicon surface-barrier detector. This detector is mounted on the conical assembly at about 35 cm from the tritium target and at a 174° angle from the D+ beam line. A typical shape for the spherical assemblies is shown in Fig. 1. Dimensions, weights and densities of the targets are given in Table 1.

The neutron TOF leakage spectra have been measured in the range of 1 to 14 MeV with a 5.08 cm diameter by 5.08 cm long stilbene detector located at 26° and about 10 m from the tritium target. The detector bias was set equal to ^{22}Na 1/4 low bias (the low Na bias is defined as the Compton recoil edge of the 0.51 MeV gamma ray from a ^{22}Na source, and corresponds to an equivalent electron energy of 0.34 MeV). Pulse-shape discrimination was used to minimize the gamma-ray background, resulting in a ratio of signal (neutrons from the spherical assembly) to background (time independent neutrons and gamma-rays) of 10^4 to 10^2 between 14 and 1 MeV neutrons respectively.

The relative efficiency of the stilbene detector as a function of energy (with reference to its efficiency at 14 MeV) in the interval 1-14 MeV has been discussed earlier.[15] It is determined by measuring the neutron leakage spectrum from a polyethylene sphere (0.8 mfp CH_2), and requiring that the calculations fit the measurements. Because the shape of the efficiency curve at energies close to the bias cutoff is very sensitive to the exact setting of the pulse height threshold bias, it is necessary to repeat the CH_2 measurement each time that a new set of measurements is performed at a particular bias.

The procedure described above to determine the relative stilbene efficiency implies that the hydrogen and carbon cross sections are correctly represented in the neutron libraries[5,6]. This assumption has been checked[15] by measuring the neutron emission spectrum from the CH_2 sphere with a NE-213 detector of equal dimensions and known efficiency.[1] The Monte Carlo calculations with ENDF/B-V or ENDL are in good agreement with the measurement.

Recently we have measured[16] the absolute efficiency of the stilbene detector in the energy range 0.5 to 12 MeV, using a ^{252}Cf source. The fission fragments were detected with an argon-nitrogen (Ar-N_2) gas scintillator. The values obtained between 1 and 12 MeV are in very good agreement with those generated from the CH_2 measurement. The relative efficiency for the stilbene detector (as determined by the CH_2 pulsed sphere comparison) has been made absolute by measuring its absolute efficiency at 14.8 MeV. This has been done by comparing the the stilbene detector with a proton recoil counter (PRC) of known[17] efficiency placed at 50 cm from the tritium target. Fig. 2 shows the absolute efficiency for the stilbene detector obtained as described. The solid curve is a Monte Carlo calculation

using the code[18] NEFF4. The agreement between the measured and calculated values is better than 10% over the whole energy range, while the agreement in shape is whithin +5%. Since the pulsed sphere data are expressed as counts/ns/source count (with the sphere removed) the accuracy of the comparison with calculations is dependent upon the relative efficiency, i.e., upon the shape of the efficiency curve.

III. CALCULATIONS

The measured TOF neutron emission spectra from ^{165}Ho, ^{181}Ta, ^{197}Au, and natural Pb have been compared with Monte Carlo calculations carried out with the code[19] TART (a coupled neutron-photon transport code). This code calculates the energy and time-of-arrival of each neutron at the detector position. By folding in the detector efficiency as a function of neutron energy a calculated TOF spectrum is obtained which can be directly compared with the experimental data. In order to have an accurate representation of the 14 MeV neutron source the calculations include: a)- the anisotropy and energy variation with angle of the $^{3}H(d,n)^{4}He$ reaction, b)- the time spread of the deuteron beam burst which is obtained from the shape of the full prompt gamma peak, c)- the time resolution of the measured neutrons (1-2 ns), which includes the time spread due to the electronics and the detector resolution, and d)- the geometry and composition of the low-mass tritium target assembly[1].

The accuracy of the modeling of the 14 Mev source in the calculations can be judged from the comparison of a measured and calculated "Blank" run shown in Fig. 3, which shows the measured 14 Mev neutron peak well described by this calculation. A "Blank" run is by definition, a measurement of the TOF spectrum with the sphere removed. These runs, which alternate with those taken with the sphere in place, are used for time independent background corrections and source strength determinations (14 MeV neutron counts/alpha particle).

To test the cross section evaluations for these materials found in the ENDF/B-V and ENDL libraries[5,6], the measured TOF spectra of the emitted neutrons are compared with the calculated spectra. This is always an exact

comparison, independent of the size of the sphere and the fissionable nature of the target. These two factors contribute to an uncertainty in the transformation from time of arrival to neutron energy because of the inability to determine accurately the time at which the emitted neutron was born.[15] However, for the present set of targets, small (sphere radii << 10 cm) and non-multiplying assemblies, the transformation from measured time-of-flight spectra to energy spectra is accurate to a few percent. To facilitate the use of these measurements by other laboratories in the test of their cross sections or/and codes, the energy spectra are also given in neutrons/Mev-source neutron (Appendix).

The neutron emission spectra for the materials studied have also been calculated using cross sections generated by the code[11] ALICE/LIVERMORE 82. This code calculates single and multiple particle emission from evaporation processes[20] and precompound decay using the hybrid/geometry dependent hybrid models[21,22]. The evaporation calculation can include competition from fission according to the Bohr-Wheeler approach[23]. Optical model[24], classical sharp-cutoff algorithms[25] and the parabolic model[26] are used to calculate inverse reaction cross sections, reaction cross sections and partial reaction cross sections according to the nature of the projectile.

The reaction cross sections, the energy distributions and angular distributions of the secondary neutrons from precompound and compound processes from 2 to 20 MeV calculated by ALICE were used to replace the corresponding values in ENDL for the four materials. The resulting test library was then processed to provide input for TART to carry out the Monte Carlo calculation of the emission spectra. The elastic scattering differential cross sections in this test library have been generated using standard spherical optical model potentials. This data file, where the

elastic differential cross sections and all data associated with inelastic scattering to levels are from the ENDL library and the remaining reaction cross sections and spectra were generated with ALICE/LIVERMORE 82, will be called ALICE/Sph (Spherical OM) throughout the text.

The sensitivity of the pulsed sphere data to deformation effects arising from the nuclear shape in the calculated emission spectra was also investigated. Coupled channel (CCh) formalism for deformed nuclei and phenomenological global optical potentials optimized for neutron scattering[27,28] were used to calculate the differential elastic scattering and inelastic scattering cross sections to the low excited levels for incident neutron energies between 1 and 15 MeV. These calculations were carried out with the code ECIS79 written by Raynal[12]. A second test library was generated in which the ECIS79 calculated data in the 2-20 MeV energy interval replaced those from ENDL in the first test library. TART calculations were carried out with this second test library using the ECIS79 cross sections plus those calculated with ALICE for the compound and precompound emission. The comparison of these calculations, ALICE/CCh, vith ALICE/Sph and the measurements will be discussed for each material.

^{165}Ho Results.

The measured neutron emission spectrum from 0.8 mfp Ho has been compared with TART calculations using the ENDL, ALICE/Sph, and ALICE/CCh cross sections. As pointed out earlier, the ENDF/B-V does not have an evaluation for holmium. Holmium is a rotational nucleus characterized by a large static quadrupole deformation[27] with the value[28] of the deformation parameter β_2 = 0.320. This deformation gives rise to collective motions that result in strong coupling between the low excited levels of the ground state

rotational band and the ground state (7/2-) and between the excited levels. CCh calculations were carried out which included the ground state, the first (9/2-) and the second (11/2-) low-lying excited levels. The differences founded for the elastic differential cross sections calculated with a spherical OM potential (OMP) and the deformed OMP were mainly at angles larger than 90 degrees. The spherical OMP overestimates the backward angle scattering cross sections by factors ranging between 1.2 and 2 for angles between 90 and 180 deg. The calculated integral spectra were very close for calculations done with ALICE/Sph and ALICE/CCh, with the latter giving slightly better agreement with the measured neutron spectra above 5 MeV. In Fig. 4 the comparison between the measurements and calculations carried out with the ENDL and ALICE/Sph cross sections is shown. Both calculations reproduce the measurements fairly well, with ALICE/Sph giving an overall better fit. This is quantitatively shown in Table IIa, where the measured integrals for three energy intervals, 1-5, 5-10, and 10-15 MeV are given together with the ratios of the calculated/measured integrals obtained from each calculation for these energy intervals. The results obtained with ALICE/CCh for the 5-10 and 10-15 MeV intervals show a small improvement over the ratios obtained with ALICE/Sph for these intervals. However, since differential elastic scattering measurements for Ho were not found to show the need for a deformed OMP, the magnitude of the differences between the spherical and deformed ALICE calculations shown in Table IIa are of little practical consequence.

Since the neutron emission spectrum is sensitive mainly to the cross sections of the incident neutrons, Table IIb shows the 14 MeV cross sections used in the calculations. The large (n,n') cross section (500 mb) in the ENDL library results in the overestimation of the calculated integral in the 5-10

MeV interval by as much as 18.3 %. For holmium, the ENDL representation of the (n,n') process is totally subsumed into a continuum representation, with the energy distribution accounting for the secondary neutrons arising from excitation of the lowest lying level. The substitution in the first test library of ALICE calculations for the continuum (n,n') cross section, resulted in a lessening of the cross section from 500 to 187 mb. The inclusion of the excitation from the two low-lying levels (0.095 and 0.210 MeV excitation energy with 154 and 73 mb respectively) in the second test library from the ECIS79 calculated data brought the total (n,n') cross sections to 414 mb (227 mb from the levels plus 187 mb from ALICE), about 17% less than the ENDL value. Although it is expected that this difference could be further reduced by including higher excited levels in the CCh calculation, it does not imply that the value of the ratio - measured to calculated integral- in the 5-10 Mev interval (0.987) obtained with ALICE/CCh (Table IIa) will increase to the value of 1.183 given by ENDL. The value of these ratios reflect not only the magnitude of the cross sections, but also their energy spectra, i.e., ALICE/Sph calculation gives a value of 0.939 for the ratio with only 187 mb for the (n,n') cross section.

^{181}Ta Results.

The measurements of the neutron emission spectra from 1 and 3 mfp Ta spheres are compared with the TART calculations in Figs. 5 and 6 respectively. The calculations were carried out using the ENDF/B-V and ENDL libraries.[5,6] (See upper and middle curves) and ALICE/Sph (bottom curves). In addition, a CCh was carried out for neutrons between 1 and 15 MeV which included the GS (7/2+) and the two lowest excited levels of its rotational band, the 9/2+ and 11/2+ at 0.136 and 0.301 MeV exitation energy

respectively. The value of the quadrupole deformation parameter is 0.260. The elastic differential cross sections at 14 Mev calculated with the deformed optical potential are in better agreement with the measurements[29] than those calculated with the spherical optical potential. As found for Ho, the calculations carried out with ALICE/CCh shows small improvements over ALICE/Sph in the region of 5 to 15 MeV (Table IIIa).

From the agreement (bottom curve) shown between the calculations and measurements in Figs. 5 and 6, it can be concluded that the calculations with ALICE give an overall better representation of the measurements than those with the ENDF/B-V and ENDL libraries over the whole energy range. Table IIIa lists the measured values of the integrals for three energy intervals, 1-5, 5-10 and 10-15 MeV, and the ratios of the calculated to measured values obtained from each calculation. From these ratios, which are the indicators of the goodness of the fits to the measurements, it is concluded that all four calculations overestimate the production of neutrons in the 1-5 MeV interval. The evaluated libraries overpredict the production of neutrons in this energy interval by as much as 20 -30 %, and ALICE does it by 15-20 %. This effect seems to result mainly from the shape of the energy differential spectrum predicted for the secondary neutrons emmited from Ta when bombarded with 14 MeV neutrons. This effect can be seen in Fig. 7, where the differential energy spectrum for the secondary neutrons measured by Vonach et al.[30] at 14.1 MeV is compared with the energy spectra predicted by the ENDL library and ALICE/SPh. The measurements of Hermsdorf et al.[31], although at slighty higher energy (14.6 MeV) have also been plotted in Fig.7 in order to compare the shape of the spectrum for the higher energy neutrons with the calculations up to 14 MeV. Both calculations overestimate the spectrum between 2 and 5 MeV, but ALICE predicts lower values than ENDL for the cross sections between

1 and 3 MeV (630 to 367 ns neutron flight time). This is consistent withs he better agreement obtained with ALICE in Figs. 5 and 6 for the respective time interval. Although ALICE underpredicts the emission of neutrons above 7 MeV, the shape of the spectra (Fig. 7) is reproduced reasonably well by this calculation. This is not the case with the ENDL library, where the shape of the spectra due to emission of only one neutron is represented by a straight line between the values of 33 and 66 mb for neutrons emitted with energies in the interval 3-14 MeV. While for each individual interval the differences using the four libraries are as noticed, the integral over the whole range, 1.0-15 MeV, shows the ENDL values to be slightly, but not significantly, better in agreement with the measurements.

In Table IIIb the neutron cross sections at 14 MeV used in the above calculations are listed. The coupled channel calculation for the scattering of neutrons from the ground state, 0.136 and 0.301 excited levels gives a total of 181 mb for the inelastic neutron scattering from these levels at 14 MeV (129 and 52 mb for the 0.136 and 0.301 MeV levels respectively). This increase, together with a 10% increase in the calculated elastic cross section over the value obtained with ALICE/Sph, brings the magnitude of the total cross section into much better agreement with measured values[22]. The (n,2n) and (n,3n) cross sections calculated with ALICE between 14-20 MeV, are also in excellent agreement with the measurements of Veeser et al.[33]

^{197}Au Results.

A comparison of the calculated and measured time-of-flight spectrum for the neutron emision spectrum from a 2 mfp gold sphere pulsed with 14 MeV neutrons is shown in Fig. 8. The calculation carried out with the ENDF/B-V is shown in the upper curve. It badly underestimates (70%) the production of

neutrons in the 10-5 MeV interval (200 to 375 ns). This large disagreement was quite often[34] found in earlier comparisons between calculations carried out with the ENDF/B-III and measurements for materials with A > 24. It resulted from the omission of pre-equilibrium processes in the reaction mechanisms describing the interaction of the 14 MeV neutrons with nuclei. The subsequent versions of the library, ENDF/B-IV and V, have corrected this problem for most of the nuclei, although this discrepancy persists for some cases[2], as in the present case for gold.

The calculation with the ENDL library (center curve) gives an overall good representation of the measured spectra, while the calculation with ALICE/Sph (lower curve) underestimates the neutron production in the 10-5 Mev interval by about 12% (See Table IVa). Both calculations reproduce the 5-1 MeV interval rather well, giving values of 1.012 and 0.995 with a 5% error for the ratios of the calculated to measured integrals. This agreement is also reflected in the fits obtained to the differential neutron emission spectrum measured by Vonach et al.[30] (integrated over angle) with the ENDL and ALICE cross sections (Fig. 9). Below 4 MeV both calculations fit the measurements quite well. As in the case for Ta, ALICE under-predicts the emission of neutrons above 6 MeV although the shape of the spectrum is reasonable. The ENDL library accounts for the higher energy neutrons by a spectrum which is based in general systematics and reproduces reasonably well the magnitude of the measured integral spectrum.

An attempt to improve the results obtained with ALICE/Sph by performing a CCh calculation for the elastic and inelastic scattering from the low-lying excited levels in Au was not successful (Table IVa). Assuming a weak coupling model[35], these levels are described by the coupling of the odd $d_{3/2}$ proton to the g.s. (0+) and 2+ excited states, respectively, of the ^{196}Pt core.

The CCh calculation included the g.s.(3/2+), the 0.077 MeV (1/2+), the 0.269 MeV (3/2+), and 0.279 MeV (5/2+) excited levels. The value[28] used for the deformation parameter of the ^{196}Pt core was $\beta_2 = 0.125$. At 14 Mev the calculated inelastic cross sections from these levels are 10.7, 20.3, and 29.3 mb respectively.

In Table IVb the cross sections at 14 MeV for the four calculations are given; with the exception of the values of the (n,n') cross sections where large differences exist among the calculations, the elastic and other partial cross sections differ by no more than 5%. It is interesting to point out the importance of the proper description of the differential neutron emission spectra in the calculations once more. The ENDF/B-V with a total of 298 mb assigned to the (n,n') gives a worse fit than ALICE (which has only 205 mb) to the measured spectrum between 5-10 MeV (Fig. 8). As discussed earlier, the ENDF/B-V file for gold describes the total (n,n') cross section only as the result of a compound process where the neutrons are emitted with an average energy of 1-2 MeV.

Pb Results.

The neutron emission spectrum from 1 mfp natural lead is compared in Fig. 10 with calculations carried out with the ENDF/B-V and ENDL cross section libraries (upper and center curves) and cross sections generated with the ALICE code (lower curve). The best agreement is obtained with the ENDL calculation which gives values very close to one for the ratios between the calculated and measured integrals (Table Va). The ENDF/B-V underpredicts the total neutron emission in the 1-5 MeV interval by as much as 20%. This could be the result of assigning too large a fraction of the total (n,n') cross section to the discrete levels, 121 mb versus 239 mb to the continuum (Table

Vb). However it should be noticed that this calculation gives the best fit to the measured spectrum in the time interval 180 to 220 ns (12-9 MeV). The neutron energies correspond to excitation energies to around 5 MeV in the Pb nucleus. The ENDF/B-V library[5] has a total of 11 levels in this energy interval corresponding to excited levels in the ^{206}Pb, ^{207}Pb and ^{208}Pb isotopes and among which is distributed the 121 mb (n,n') cross section. The 400 mb assigned to the (n,n') cross section (Table Vb) in the ENDL library are assumed instead to be the contribution from the pre-equilibrium process to this cross section and the energy distribution is represented [as in the case of Ta (Fig. 7)], by an straight line between 3.5 and 13.5 MeV with 27 and 54 mb respectively. The inability of the ENDF/B-V to fit 5-10 MeV region lies in the shape of the energy distribution for the secondary neutrons, since the magnitude of the (n,2n) cross section is the same in both libraries. In the ENDF/B-V a large fraction of the emitted neutrons has energies below 1 Mev. This effect is already visible in Fig. 10 at neutron flight times larger than 600 ns. A similar problem is encountered in the calculations carried out with the cross sections generated with the code ALICE. In Fig. 11 the measured energy differential spectrum[30] is compared with two ALICE calculations. The dashed line has been obtained using the value of the level density parameter[20] ,a, equal to the its default value in the code[11], a = A/9, with A = 208. The solid line has been obtained with a = A/16. This lower value of a corresponds to a higher nuclear temperature [$\theta = (E/a)^{1/2}$], shifting the energy spectrum of the secondary neutrons toward higher energies. This effect can be clearly observed in Fig. 11 and brings the calculation in much better agreement with the measurements. The Monte Carlo calculations shown in Fig. 10 (lower curve) were done using the lower value of the density parameter a = A/16. This value gave a ratio for the

calculated/measured integrals in the 5-1 Mev energy interval of 0.760 (Table Va), which should be compared with a value of 0.650 for a = A/9. The latter value was chosen as a default option in ALICE because of the good agreement obtained in the comparisons with experimental measurements[36] of neutron and proton emission spectra. The need for a harder neutron emission spectrum in Pb is found in the nuclear structure of this nucleus: ^{208}Pb is a closed shell nucleus where single particle levels become important in the calculation of the level density[37]. They will account for the presence of a larger fraction of higher energy neutrons than that predicted by the expression[20] of the level density used in ALICE. The value of a = A/16, and even a smaller value of A/20, fit the measured spectra much better.

Although ^{208}Pb is a good example of a spherical nucleus, it is also a good vibrational nucleus. A CCh calculation was carried out including the GS (0+) and 2.615 MeV (3-) level with a coupling constant[38] β_3 = 0.130 for incident neutron energies between 1 and 15 MeV. Noticeable improvement over ALICE/Sph calculation in the fit to the measured spectrum for neutron energies below 10 MeV was observed. The values of the ratios obtained from ALICE/CCh (Table Va) for the intervals 1.0-5.0 and 5.0-10 Mev are 0.857 and 0.972 respectively, compared to 0.760 and 0.814 given by ALICE/Sph.

IV. SUMMARY

Measurements of the neutron emission spectra in the 1 to 15 MeV energy interval from Ho (0.8 mfp), Ta (1.0 and 3.0 mfp), Au (1.9 mfp), and Pb (1.0 mfp) have been made at 14 MeV using the pulsed sphere transmission and time-of-flight (TOF) techniques. These data have been compared with Monte Carlo calculations carried out with the neutron-photon transport code[19] TART for two evaluated neutron libraries[5,6], the ENDF/B-V and ENDL. In addition, two "test neutron libraries" ("ALICE/Sph and ALICE/CCh) were generated where the precompound and compound cross sections were obtained from nuclear model calculations using the code[11] ALICE/LIVERMORE 82. In the first test library, ALICE/Sph, these cross sections together with the reaction cross sections generated by ALICE, were substituted for the respective data in ENDL, retaining the elastic and inelastic to low-lying levels cross sections existing in this library. Collective effects due to nuclear deformations were included in the second test library, ALICE/CCh, by carrying out a coupled channel (CCh) calculation which included the elastic and inelastic differential cross sections from the low lying excited levels in the target nuclei. These cross sections, generated with the code[12] ECIS 79, replaced the ENDL data in the first test library. From the comparisons of the calculated TOF spectra with the data it can be concluded: a) From the two evaluated libraries, ENDL gives consistently better agreement with the measured TOF spectra than ENDF/B-V. The worst discrepancy obtained with the latter library is for the gold spectrum in the 5 to 10 MeV interval, where the calculation underestimates the neutron emission by as much as 80%. b) With the exception of lead, surprisingly good agreement with the measurements have been found using the cross sections generated by the "test" libraries. The

main attraction of these libraries is that only default parameters are used in the calculations, which have been obtained from the use of precompound[13,14] and compound[20-24] nuclear models over a wide range of mass and energy values. The calculations carried out for ^{208}Pb, underestimated the neutron production by about 23% in the 1 to 10 MeV interval when the default value for the level density parameter of a = A/9 was used. A value as small as A/20 is needed to reproduce the data (calculations with a = A/16 are shown in Fig. 10), which implies a harder neutron emission spectrum than that predicted by the Weisskopf's level density[19] expression used in ALICE. It is expected that this effect results from the closed shell structure of Pb, where single particle levels must be included[37] in the calculation of the level density. This effect will be tested in future calculations. c) The introduction of collective effects in the calculation of the elastic and inelastic scattering from low lying excited states improved the agreement with the data in the 1.0 to 10 MeV interval. Tables IIa, IIIa, and Va show that the ratios of calculated to measured integrals in the above interval obtained with ALICE/CCh are better than those obtained with ALICE/Sph. For gold (Table IVa) this was not the case, possibly as a result of the weak coupling model[35] used in the CCh calculations. However, since only a modest improvement was brought in general into the comparisons of the calculated and measured integral spectra by the inclusion of collective effects, it was not found advantageous to try other coupling models[38] for gold.

Neither of the two test libraries should be regarded as "new evaluations" for any of the four materials described in this work. We chose to substitute in the ENDL library, for the existing values of the cross sections, the corresponding values calculated by ALICE/LIVERMORE 82 and ECIS 79 as described in the text. This was to test the theoretical cross section data using the

calculations carried out with the test libraries and the measurements. This process could be considered a first step in producing "new evaluations" but much more work is needed before a re-evaluation would be completed. Because of the quality of the results obtained with these "test libraries" it seems that using the theoretical data will be justified when new evaluations for the materials are undertaken.

*Work performed under the auspices of the U.S. Department of Energy by the Lawrence Livermore National Laboratory under contract number W-7405-ENG-48.

APPENDIX

The measured time of flight spectra of the emitted neutrons have been transformed[1] to energy spectra by calculating the energy relativistically from the time of arrival t_i of the neutrons.

$$E_i = 939.6\ [1 - ((L/t_i c)^2]^{-1/2} - 1)$$

Where L is the distance from the center of the sphere to the face of the detector. Unfolding the detector efficiency from the time spectra and using the differential energy spectrum for the source neutrons, the energy spectrum is obtained from the above formula in units of neutrons per MeV per 14 MeV source neutron (Table VI).

FIGURE CAPTIONS

Fig. 1. Spherical target typical geometry. The dimensions are in centimeters.

Fig. 2. Measured efficiency of the 5.08 cm diameter by 5.08 cm long stilbene detector for 1/4 low Na bias (+++) and high Na bias (ΔΔΔ). The solid curves have been obtained from Monte Carlo calculations carried out with the code NEFF4 (Ref. 18).

Fig. 3. Comparison of measured and calculated neutron TOF spectra from a "Blank" run (no spherical target positioned at the tritium target). The small peak at ∿360 ns corresponds to 2.81 MeV neutrons from the $^{2}H(d,n)^{3}He$ reaction which results from the deuterium contamination of the tritium target.

Fig. 4. Comparison of measured (xxx) and calculated (——) neutron TOF spectra for 1.0 mfp ^{165}Ho. The upper calculated curve has been obtained with the ENDL library, and the bottom one with the test library ALICE/Sph.

Fig. 5. Comparison of measured (xxx) and calculated (——) neutron TOF spectra for 1.0 mfp ^{181}Ta. The calculations have been carried out with the ENDF/B-V (upper curve), ENDL (middle curve), and ALICE/Sph (bottom curve) libraries.

Fig. 6. As in Fig. 5 for 3.0 mfp ^{181}Ta.

Fig. 7. Comparison of measurements (Ref. 30, —; Ref. 31, -xx-) and calculations of the neutron emission spectra from ^{181}Ta at 14.1 MeV. The solid and dashed line have been calculated with the ENDL and ALICE/Sph libraries respectively.

Fig. 8. As in Fig. 5 for 2.0 mfp ^{197}Au.

Fig. 9. As in Fig. 7 for ^{197}Au.

Fig. 10. As in Fig. 5 fo 1.0 mfp Pb

Fig. 11. Comparison of measurements (Ref. 30,—; Ref. 31, **) of the neutron emission spectrum from Pb at 14.1 MeV with calculations carried out with ALICE/Sph. The difference between the solid and dashed curves is in the value of the level density parameter (a) used in the calculations: a = A/16 (solid curve) and A/9 dashed curve.

Table I

Physical Parameters of the Spherical Assemblies*

Material	Density [g/cm^3]	Radius [cm]	Weight [Kg]	mfp at 14 MeV
Ho	8.78	4.60	3.54	0.8
Ta	16.60	3.40	2.28	1.0
		10.20	72.20	3.0
Au	19.29	6.21	18.50	1.9
Pb	11.34	5.60	7.79	1.0

* Detailed geometry of the conical cavity to position the tritium target at the center of the sphere is given in Ref. 1.

Table IIa. Measured integrals* for 0.8 mfp ^{165}Ho and ratios of calculated-to-measured integrals.

ΔE [MEV]	Experiment ±5%	R(ENDF/B-V)	R(ENDL)	R(ALICE/Sph)	R(ALICE/CCh)
1.- 5.	0.230	---	1.134	1.104	1.104
5.-10.	0.023	---	1.183	0.939	0.987
10.-15.	0.727	---	0.999	0.985	0.990
1.-15.	0.980	---	1.034	1.021	1.017

* In units of neutron counts (sphere in) divided by the total number of 14 MeV source counts (sphere out). The errors in the ratios are also 5%.

Table IIb. Neutron cross sections [mb] for ^{165}Ho at 14 MeV.

Library	σ_T	σ_{el}	$(n,n')_{lev}$	(n,n')	(n,2n)	(n,p)	(n,α)	(n,γ)
ENDL	5174	2817	---	500	1850	---	---	7
ALICE/Sph	5032	2817	---	187	2009	13	---	7
ALICE/CCh	5246	2803	227	187	2009	13	---	7

Table IIIa. Measured integrals* for 1.0 and 3.0 mfp Ta and ratios of calculated-to measured integrals

#mfp	ΔE [MeV]	Experiment* ±5%	R(ENDF/B-V)	R(ENDL)	$R(ALICE_{Sph}$	$R(ALICE)_{CCh}$
1	1.- 5.	0.256	1.281	1.230	1.152	1.148
	5.-10.	0.024	0.975	1.107	1.045	0.984
	10.-15.	0.618	1.047	1.024	1.071	1.083
	1.-15.	0.898	1.115	1.088	1.096	1.102
3	1.- 5.	0.316	1.259	1.266	1.196	1.209
	5.0-10	0.027	0.970	1.118	0.908	0.930
	10.-15.	0.278	0.860	0.813	0.950	0.971
	1.-15.	0.621	1.068	1.056	1.074	1.090

*In units of neutron counts (sphere in) divided by the total number of 14 MeV source counts (sphere out). The error in the ratios is also 5%.

Table IIIb. Neutron cross sections [mb] for ^{181}Ta at 14 MeV

Library	σ_T	σ_{el}	$(n,n')_{lev}$	(n,n')	(n,2n)	(n,p)	(n,α)	(n,γ)
ENDF/B-V	5378	2950	40	190	2190	4	---	4
ENDL	5355	2593	33	512	2212	4	---	1
ALICE/Sph	4956	2594		214	2134	13	---	1
ALICE/CCh	5360	2817	181	214	2134	13	---	1

Table IVa. Measured integrals* for 1.9 mfp ^{197}Au and ratios of calculated-to-measured integrals

ΔE [MeV]	Experiment* ±5%	R(ENDF/B-V)	R(ENDL)	$R(ALICE)_{Sph}$	$R(ALICE)_{CCh}$
1.- 5.	0.424	1.012	1.012	0.995	1.040
5.-10.	0.032	0.281	1.041	0.880	0.852
10.-15.	0.409	0.883	0.963	0.990	0.985
1.-15.	0.865	0.923	0.994	0.988	1.007

*In units of neutron counts (sphere in) divided by the total number of 14 MeV source counts (sphere out). The error in the ratios is also 5%.

Table IVb. Neutron cross sections [mb] for ^{197}Au at 14 MeV

Library	σ_T	σ_{el}	$(n,n')_{1ev}$	(n,n')	(n,2n)	(n,p)	(n,α)	(n,γ)
ENDF/B-V	5241	2607	---	298	2333	2	0.3	1
ENDL	5282	2750	---	400	2120	2	0.3	10
ALICE/Sph	5217	2750	---	205	2250	2	0.3	10
ALICE/CCh	5350	2823	60	205	2250	2	0.3	10

Table Va. Measured integrals* for 1.0 Pb and ratios of calculated-to-measured integrals

ΔE [MeV]	Experiment* ±5%	R(ENDF/B-V)	R(ENDL)	$R(ALICE)_{Sph}$	$R(ALICE)_{CCh}$
1.- 5.	0.529	0.813	0.920	0.760	0.857
5.-10.	0.034	1.036	0.985	0.814	0.972
10.-15.	0.660	0.989	0.982	0.976	0.977
1.-15.	1.223	0.914	0.955	0.878	0.925

*In units of neutron counts (sphere in) divided by the total number of 14 MeV source counts (sphere out). The error in the ratios is also 5%.

Table Vb. Neutron cross sections [mb] for Pb at 14 MeV

Library	σ_T	σ_{el}	$(n,n')_{1ev}$	(n,n')	(n,2n)	(n,p)	(n,α)	(n,γ)
ENDF/B-V	5395	2899	121	239	2134	---	---	1
ENDL	5492	2940	---	400	2150	---	---	2
ALICE/Sph	5452	2944	---	197	2310	---	---	1
ALICE/CCh	5175	2640	28	197	2310	---	---	1

Table VI. Neutrons/MeV-Source neutron calculated from the measured neutron time-of-flight spectra.

E[1 MeV]	Ho [1 mfp] x10^{-3}	Ta [1 mfp] x10^{-3}	Ta [3 mfp] x10^{-3}	Au [2 mfp] x10^{-3}	Pb [1 mfp] x10^{-3}
1 - 2	6.504	7.284	10.397	13.000	12.830
2 - 3	2.902	2.937	3.141	4.587	7.462
3 - 4	1.208	1.239	1.290	1.863	2.992
4 - 5	0.606	0.615	0.670	0.897	1.294
5 - 6	0.382	0.395	0.429	0.527	0.636
6 - 7	0.343	0.355	0.398	0.460	0.471
7 - 8	0.285	0.295	0.332	0.382	0.367
8 - 9	0.272	0.290	0.330	0.382	0.397
9 - 10	0.274	0.309	0.346	0.401	0.437
10 - 11	0.274	0.320	0.355	0.379	0.393
11 - 12	0.286	0.323	0.320	0.354	0.330
12 - 13	0.411	0.428	0.313	0.382	0.375
13 - 14	1.026	1.194	0.674	0.805	0.852
14 - 15	53.797	45.127	19.690	29.559	48.727

REFERENCES

1. C. Wong, J. D. Anderson, P. Brown, L. F. Hansen, J. L. Kammerdiener, C. Logan, and B. A. Pohl, "Livermore Pulsed Sphere Program Summary Through July 1971". UCRL-51144, Rev. 1. Lawrence Livermore Laboratory (1972).

2. L. F. Hansen, C. Wong, T. T. Komoto, and B. A. Pohl. Nucl. Tech. 51, 70 (1980).

3. L. F. Hansen, T. T. Komoto, B. A. Pohl, and C. Wong, "Summary of Measurements and Calculations of Neutrons and Gamma-Ray Emission Spectra from Spheres Pulsed with 14 MeV Neutrons". UCID-19604, (1982).

4. "Evaluation of Magnetic Confinement Fusion Engineering Opportunities on Existing and Planned Facilities". EPRI AP-2489, July 1982.

5. ENDF/B-V Ta (Mat. 1285). Evaluated by R. J. Howerton, S. T. Perkins, R. C. Haight and M. H. Mc.Gregor (1975). ENDF/B-V Au (Mat. 1379). Evaluated by S. F. Mughabghab (1977). ENDF/B-V Pb (Mat. 1382). Evaluated by C. Y. Fu and F. G. Perey (1978).

6. ENDL, Lawrence Livermore Laboratory (LLL) Evaluated Nuclear Data Library. Evaluated by R. J. Howerton et al., UCRL-50400, Vol. 15, Parts A to E (1975-1978). The version of ENDL used for the calculations described here was of the vintage of 1984.

7. R. J. Howerton. Private communication. April 6, (1983).

8. R. C. Haight, M. M. MacGregor, R. J. Howerton, E. F. Plechaty, and L. F. Hansen. "A Comparison of ENDF/B-III Evaluated Data Sets with Pulsed Sphere Measurements". UCRL-74092, (1972).

9. L. F. Hansen, J. D. Anderson, R. J. Howerton, J. L. Kammerdiener, C. M. Logan, E. F. Plechaty, and C. Wong. Nucl. Sci. & Eng. 51, 278 (1973).

10. C. Y. Fu, Computer Code NNNGAM, ORNL (1973).

11. M. Blann and J. Bisplinghoff. Code ALICE/LIVERMORE 82. UCID-19614 (1982).

12. J. Raynal, "The Structure of Nuclei". Course on Nuclear Theory given in Trieste. Sponsored by the International Atomic Energy Egency, Vienna (1979).

13. M. Blann, Phys. Rev. Lett. 27, 337 (1971); 27, 700(E) (1971); 27, 1550(E) (1971).

14. J.J. Griffin, Phys. Rev. Lett. 28, 757 (1972).

15. L. F. Hansen, C. Wong, T. T. Komoto, E. Goldberg, R.J. Howerton, and W.M. Webster, Nucl. Sci. Eng. 72, 35 (1979).

16. B. A. Pohl, R. C. Haight, L. F. Hansen, C. Wong, "Measurements of the Absolute Efficiencies of a 2"*2" NE-213 and Stilbene Detectors Using a 252Cf Source". Unpublished.

17. H. H. Barschall, Rex Booth, C. Wong. "Neutron Flux Measurement at RTNS Facility". UCID-17206 (1976).

18. G. Dietze, private communication Feb. (1982). Phys.-Tech. Bundesanstalt Braunschweig.

19. E. F. Plechaty and J. R. Kimlinger, "TART Coupled Neutron-Photon Monte Carlo Transport Code", UCRL-50400, Vol. 14, Lawrence Livermore Lab. (1975).

20. V. F. Weisskopf and D. H. Ewing, Phys. Rev. 57, 472 (1940).

21. M. Blann, Phys. Rev. Lett. 27, 337 1971.

22. M. Blann, Phys. Rev. Lett. 28, 757 (1972).

23. N. Bohr and J. R. Wheeler, Phys. Rev. 56, 426 (1939).

24. M. Blann and T.T. Komoto, " Alert I and II, Hauser-Feshbach Codes for Nuclei at High Excitation and Angular Momenta", LLNL report UCID-19390 (1982). Unpublished.

25. M. Blann, Phys. Rev. C 21, 1770 (1980).

26. T. D. Thomas, Phys. Rev. 116, 703 (1959).

27. A. Bohr and B. R. Mottelson, "Nuclear Structure", V.2 Edit. by W. A. Benjamin, Inc. (1975).

28. P. H. Stelson and L. Grodzins, Nucl. Data Sect. A 1, 21 (1965).

29. L. F. Hansen, F. S. Dietrich, B. A. Pohl, C. H. Poppe, and C. Wong, Phys. Rev. C 31 (1985). See other references in this paper.

30. H. Vonach, A. Chalupka, F. Wenninger, G. Staffel, "Measurements of the angle-integrated secondary neutron spectra from interaction of 14 MeV neutrons with medium and heavy nuclei", BNL-NCS-51245-Vol 1,343, (1980).

31. D. Hermsdorf, A. Meister, S. Sassonoff, D. Seeliger, K. Seidel and F. Shanin, "Differentielle Neutronemissionquerschnitte bei 14.6 MeV Einschubenergie fur die Elemente Be, C, Na, Mg, Al, Si, P, S, Ca, Ti, V, Cr, Mn, Fe, Co, Ni, Cu, Zn, Ga, Se, Br, Zr, Nb, Cd, In, Sn, Sb, I, Ta, W, Au, Hg, Pb, und Bi" INDC(GDR)-2/L (1975).

32. D. G. Foster, Jr. and D. W. Glasgow, Phys. Rev. C3, 576 (1971).

33. L. R. Veeser, E. D. Arthur, and P. G. Young, Phys. Rev. C16, 1792 (1977).

34. L. F. Hansen, C. Wong, T. T. Komoto, J. D. Anderson, Nucl. Sci.& Eng. 60, 27, (1976).

35. R. P. Sharma, Nucl. Phys. A154, 312 (1970).

36. M. Blann and K. H. Vonach, Phys. Rev. C28, 1475 (1983).

37. S. M. Grimes, "Level Density Calculations: Past, Present and Future". Proceding Conference Neutron-Nucleus Collisions: A Probe of Nuclear Structure. Burr Oak State Park, Ohio, 1984. AIP Conf. Proc. # 124.

38. R. W. Finlay, J. R. Annand, T. S. Cheema, J. Rapaport, and F. S. Dietrich, Phys. Rev. C30, 796 (1984).

39. J. P. Delaroche, "Potential Optique Nucleon ^{197}Au Entre 10 keV et 57 MeV", Proceedings of an International Conference on Neutron Physics and Nuclear Data. pp. 366-370. Harwell, England 1978.

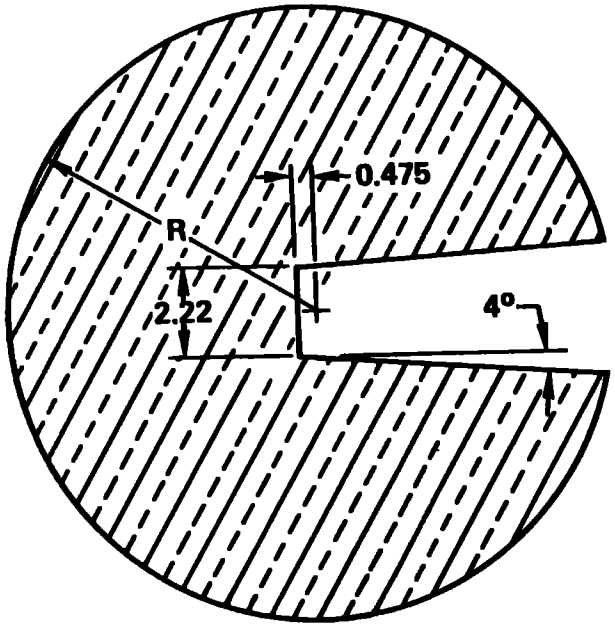

Fig. 1

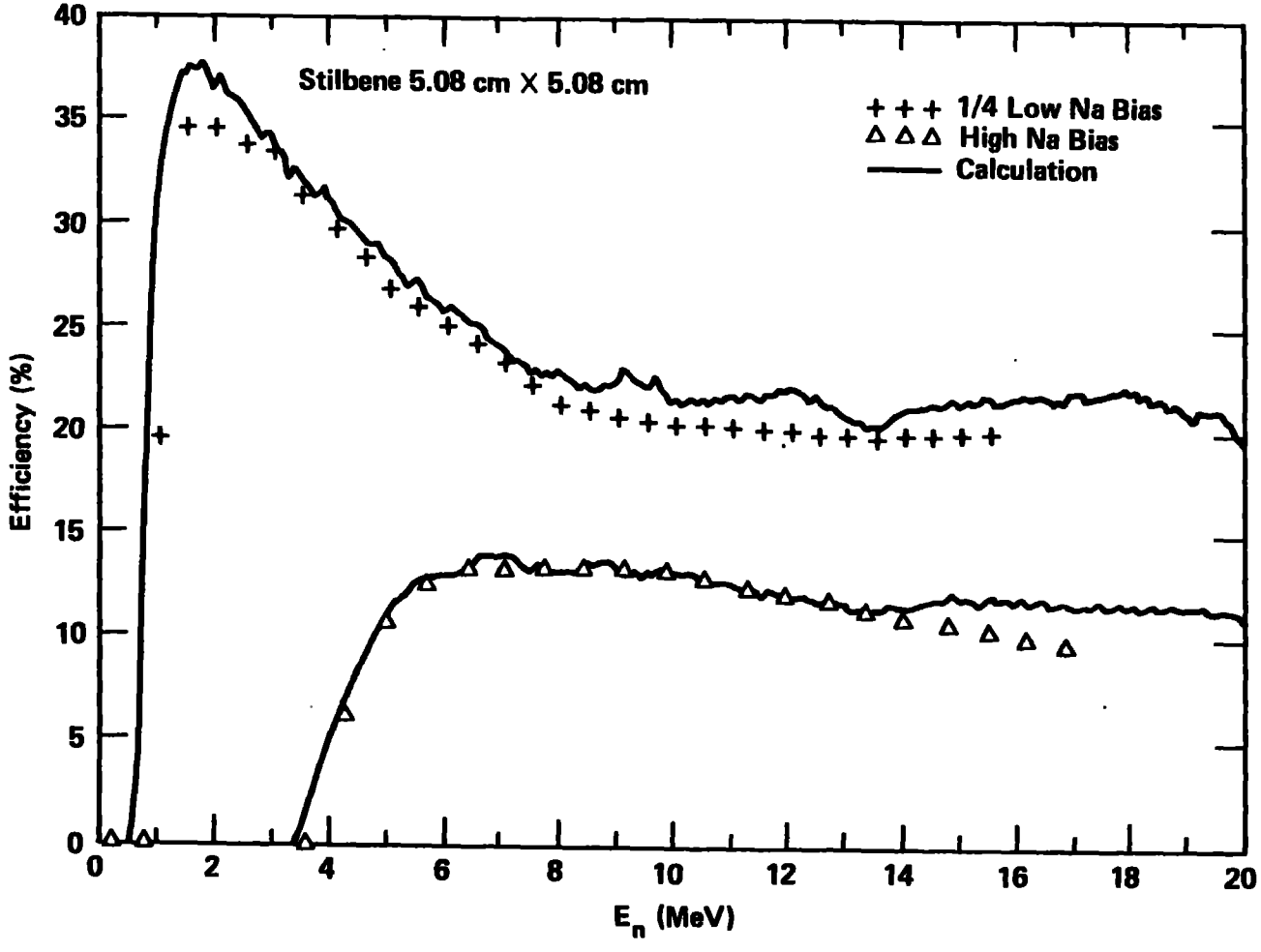
Stilbene 5.08 cm X 5.08 cm
+ + + 1/4 Low Na Bias
Δ Δ Δ High Na Bias
Calculation
Efficiency (%)
E_n (MeV)
0
5
10
15
20
25
30
35
40
0
2
4
6
8
10
12
14
16
18
20

Fig. 2

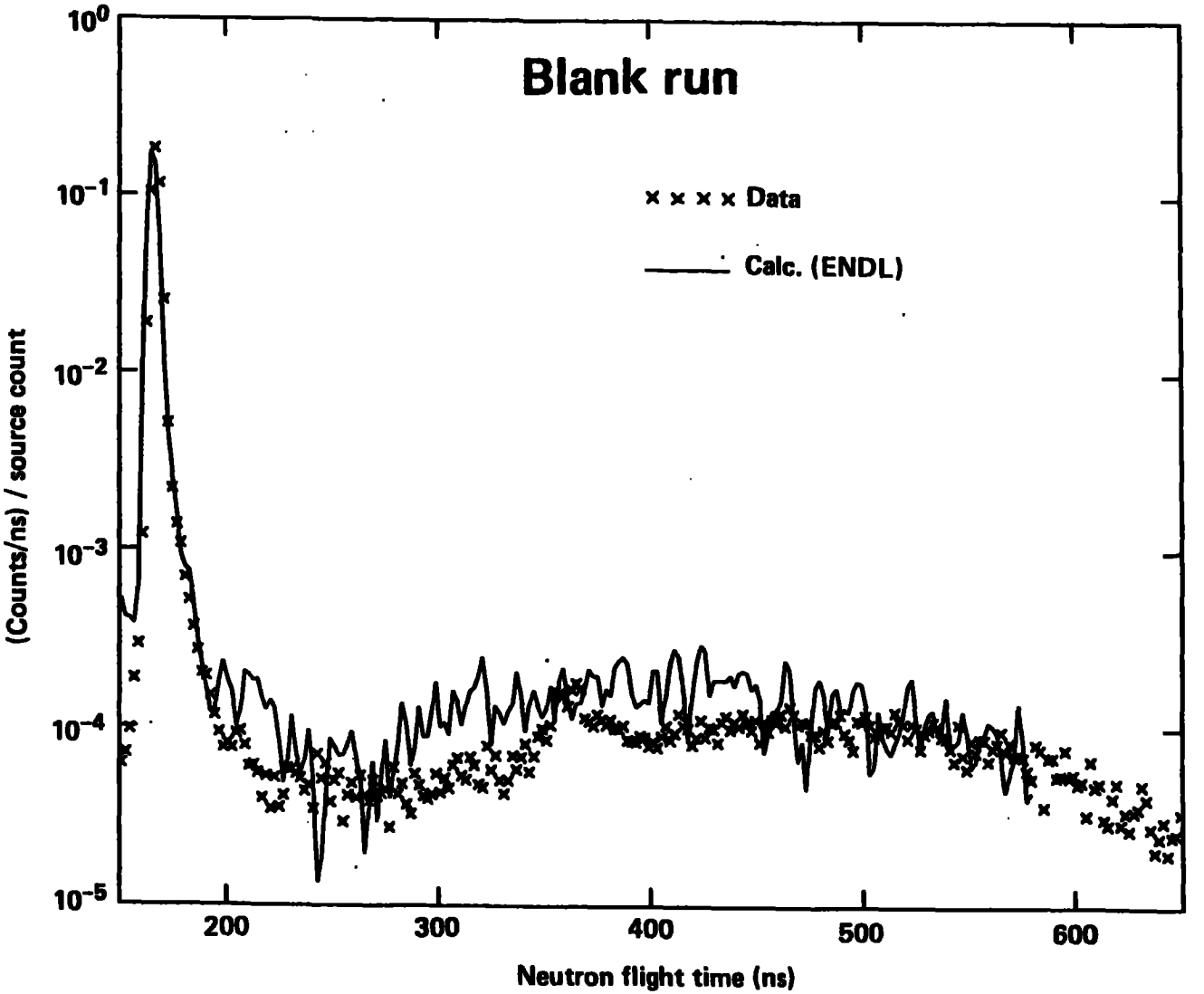
Blank run
× × × × Data
Calc. (ENDL)
(Counts/ns) / source count
Neutron flight time (ns)
10^{0}
10^{-1}
10^{-2}
10^{-3}
10^{-4}
10^{-5}
200
300
400
500
600

Fig. 3

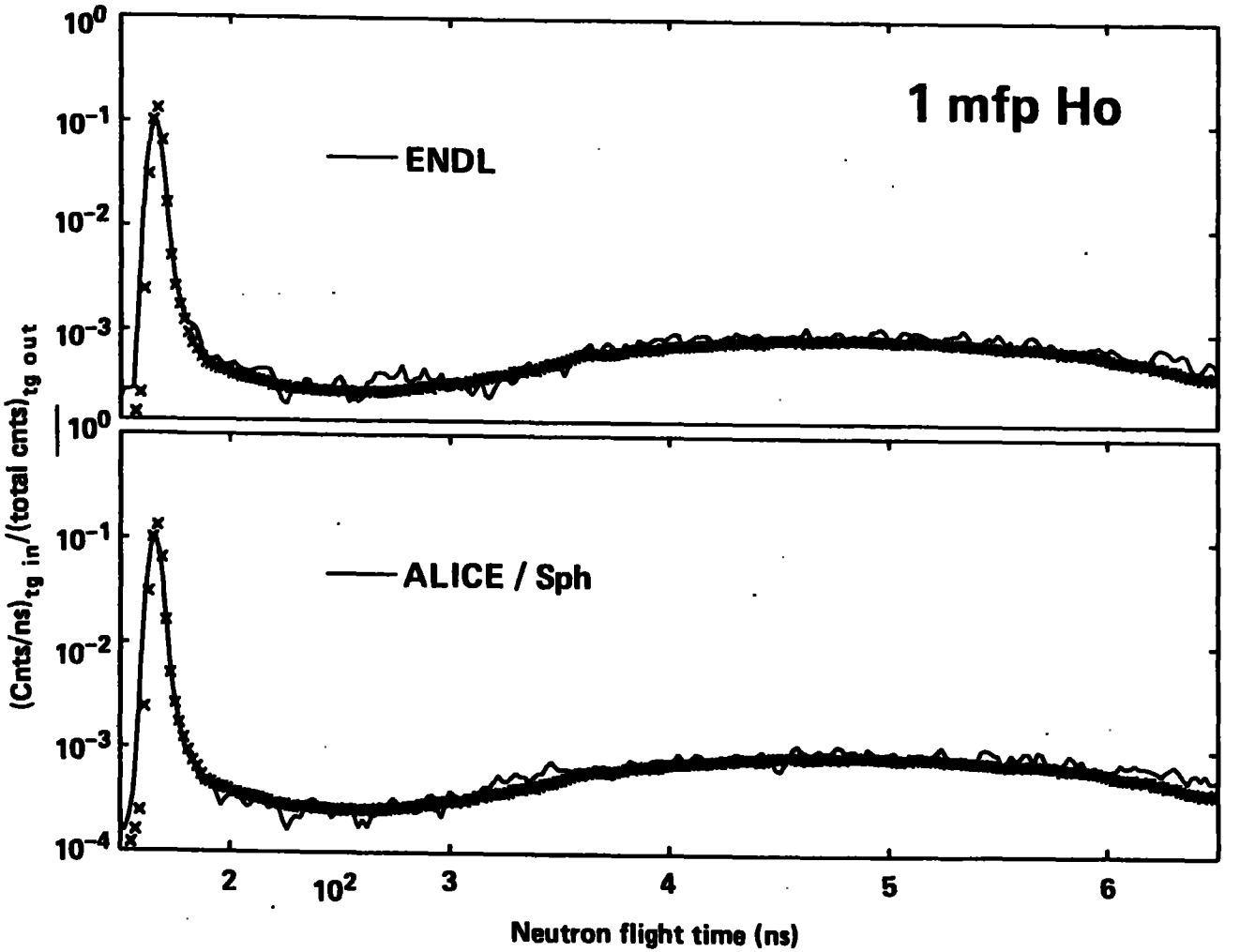
1 mfp Ho
ENDL
ALICE / Sph
10^0
10^{-1}
10^{-2}
10^{-3}
10^{-4}
2
10^2
3
4
5
6
$(Cnts/ns)_{tg\ in}/(total\ cnts)_{tg\ out}$
Neutron flight time (ns)

Fig. 4

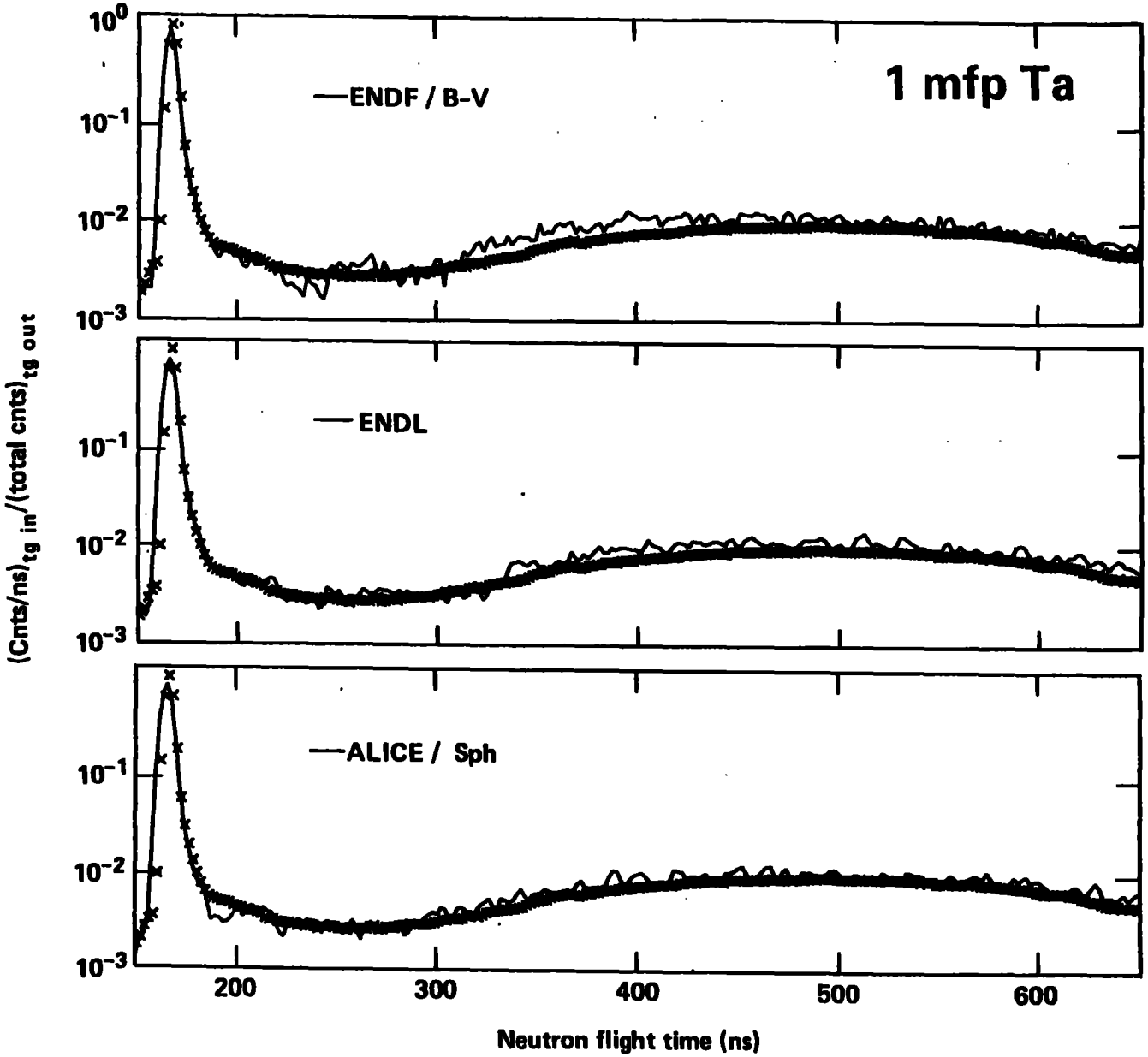
1 mfp Ta
—ENDF / B-V
— ENDL
—ALICE / Sph
10^0
10^{-1}
10^{-2}
10^{-3}
200
300
400
500
600
Neutron flight time (ns)
$(Cnts/ns)_{tg\ in}/(total\ cnts)_{tg\ out}$

Fig. 5

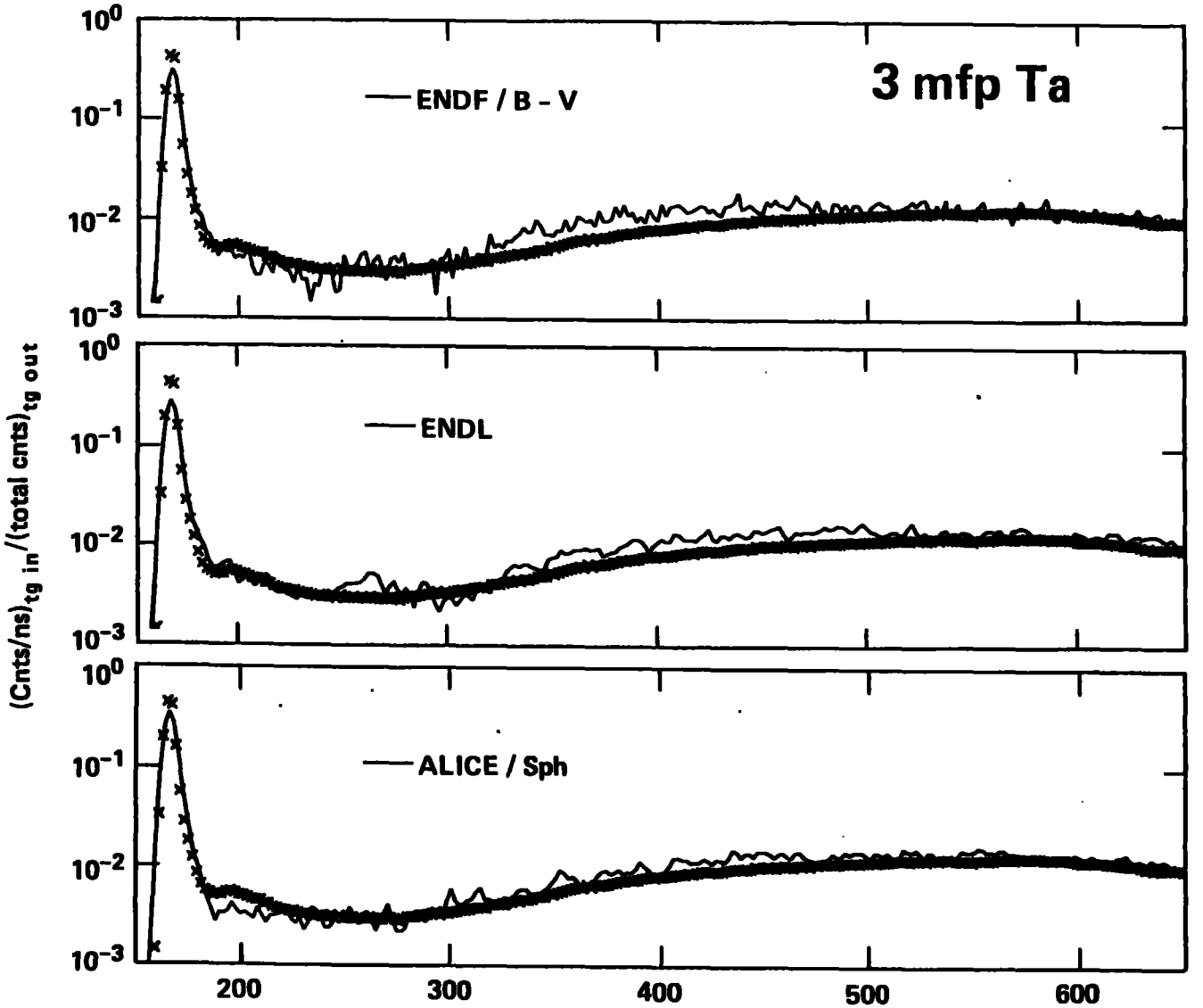
3 mfp Ta
ENDF / B - V
ENDL
ALICE / Sph
10^0
10^{-1}
10^{-2}
10^{-3}
200
300
400
500
600
$(Cnts/ns)_{tg\ in}/(total\ cnts)_{tg\ out}$

Fig. 6

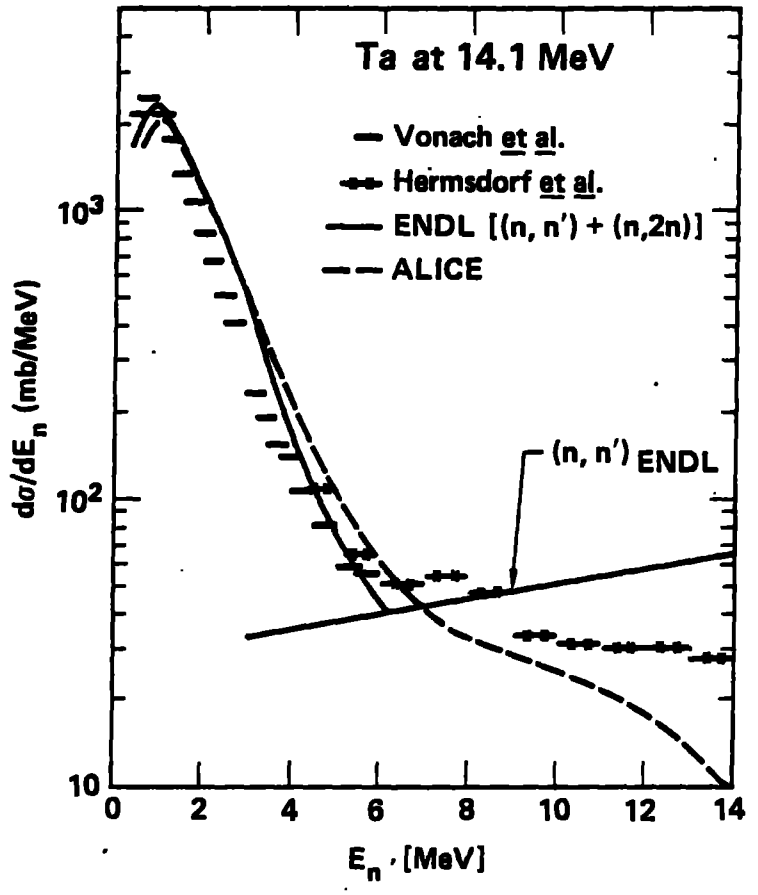
Ta at 14.1 MeV
Vonach et al.
Hermsdorf et al.
ENDL [(n, n') + (n,2n)]
ALICE
(n, n') ENDL
dσ/dE_n (mb/MeV)
10^3
10^2
10
0
2
4
6
8
10
12
14
E_n · [MeV]

Fig. 7

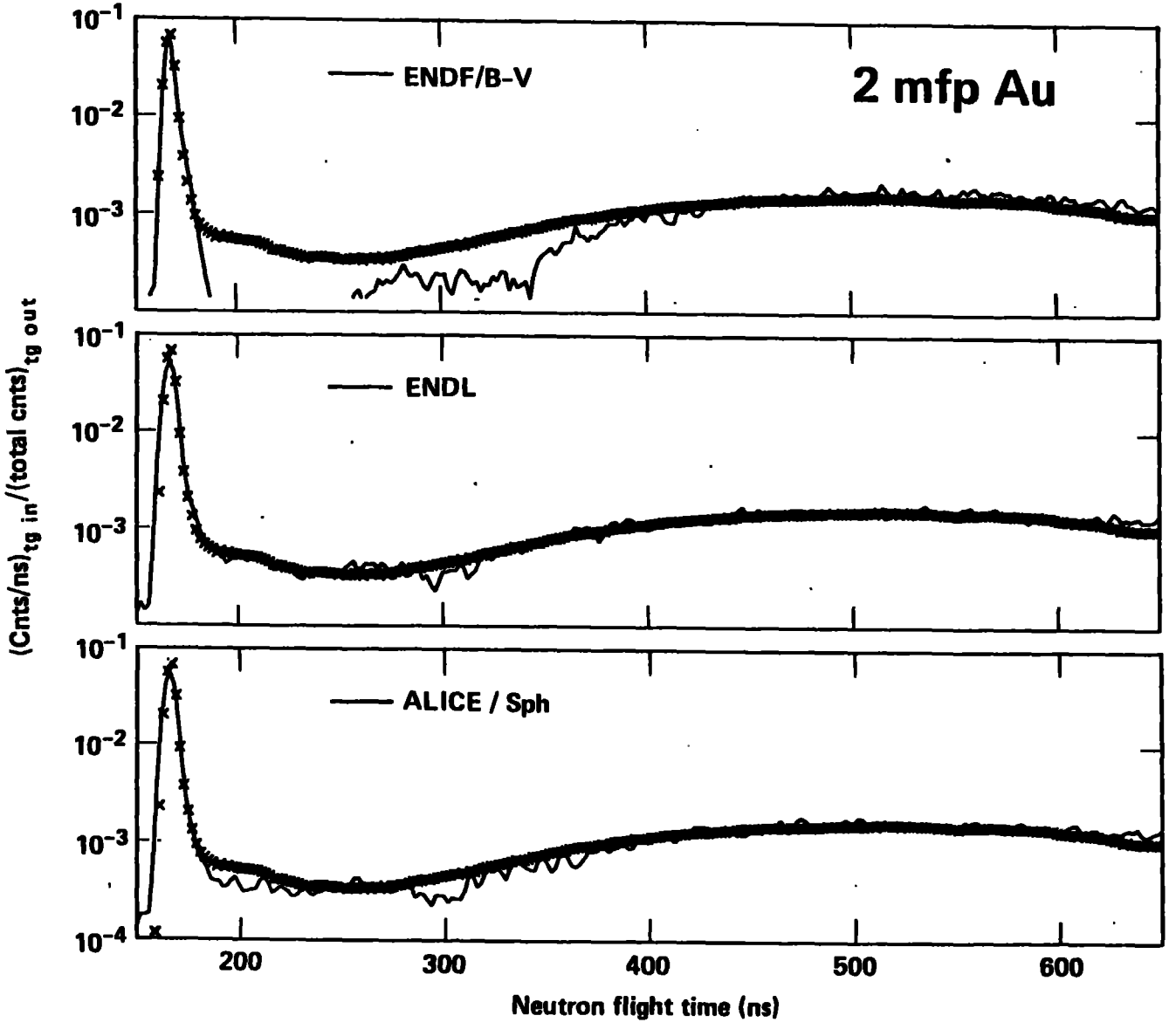
ENDF/B-V
2 mfp Au
ENDL
ALICE / Sph
10^{-1}
10^{-2}
10^{-3}
10^{-4}
200
300
400
500
600
Neutron flight time (ns)
$(Cnts/ns)_{tg\ in}/(total\ cnts)_{tg\ out}$

Fig. 8

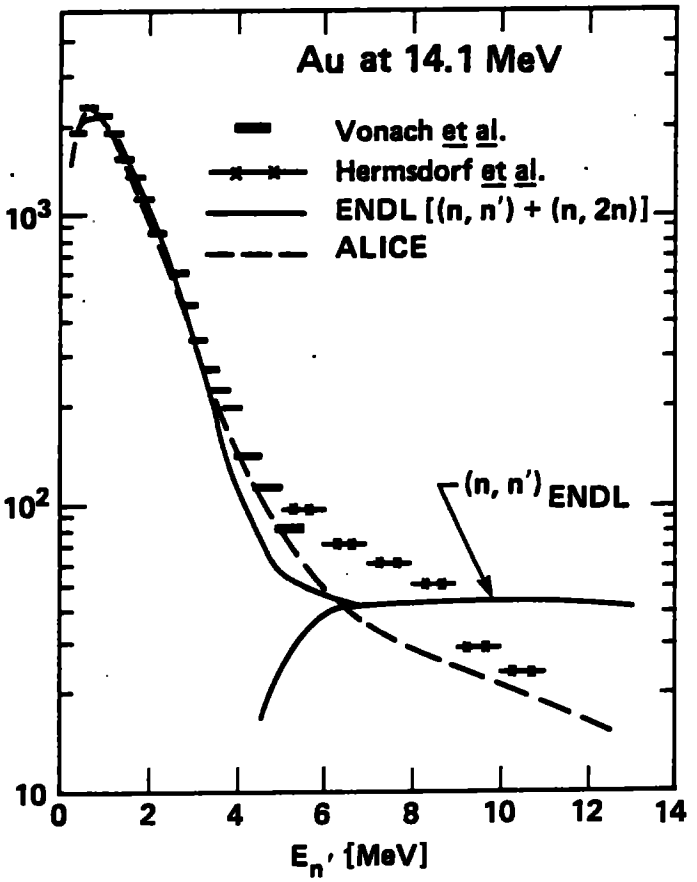
Au at 14.1 MeV
Vonach et al.
Hermsdorf et al.
ENDL [(n, n') + (n, 2n)]
ALICE
(n, n') ENDL
10³
10²
10
0
2
4
6
8
10
12
14
E_n' [MeV]

Fig. 9

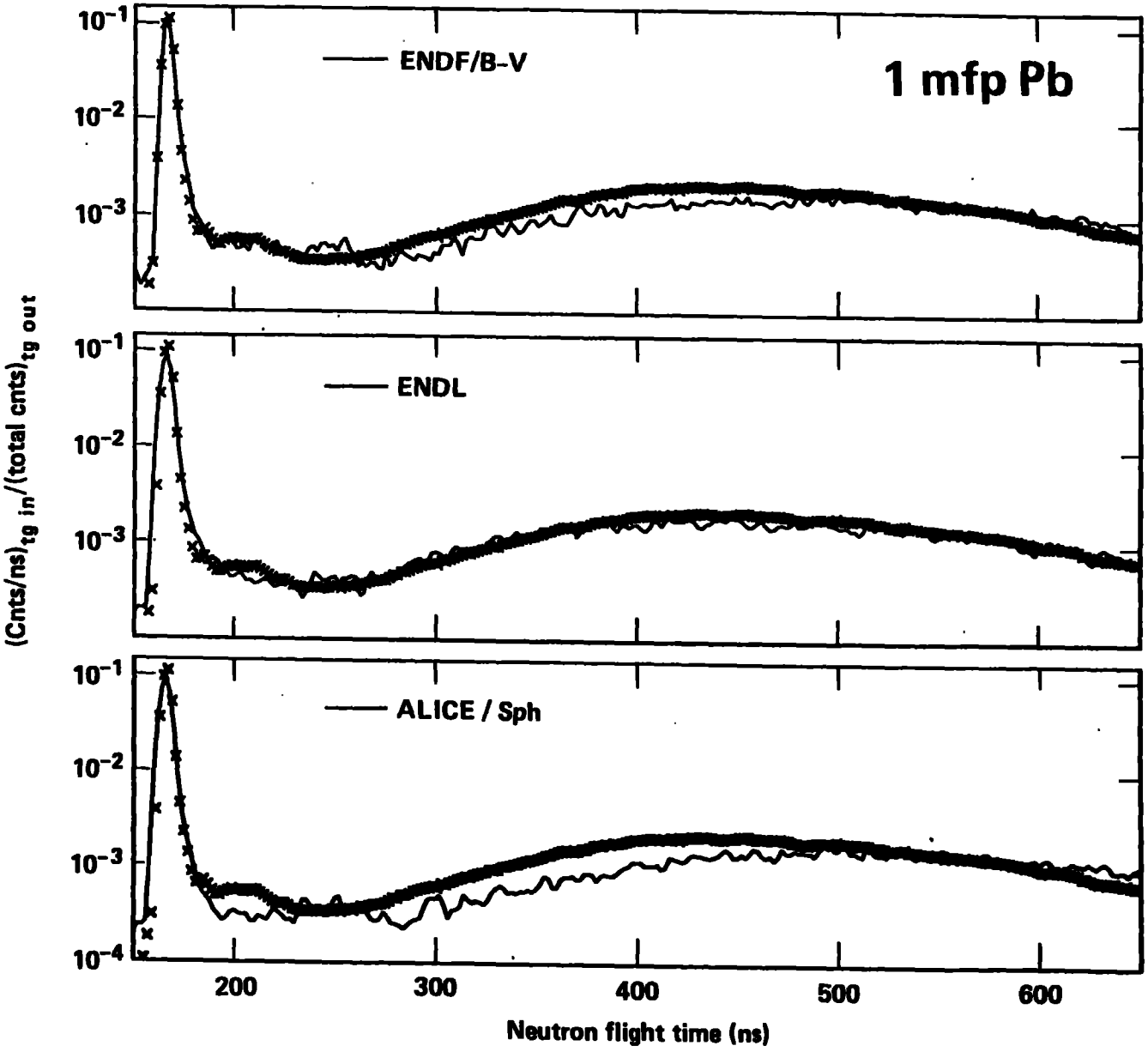
1 mfp Pb
ENDF/B-V
ENDL
ALICE / Sph
10^{-1}
10^{-2}
10^{-3}
10^{-4}
200
300
400
500
600
Neutron flight time (ns)
$(Cnts/ns)_{tg\ in}/(total\ cnts)_{tg\ out}$

Fig. 10

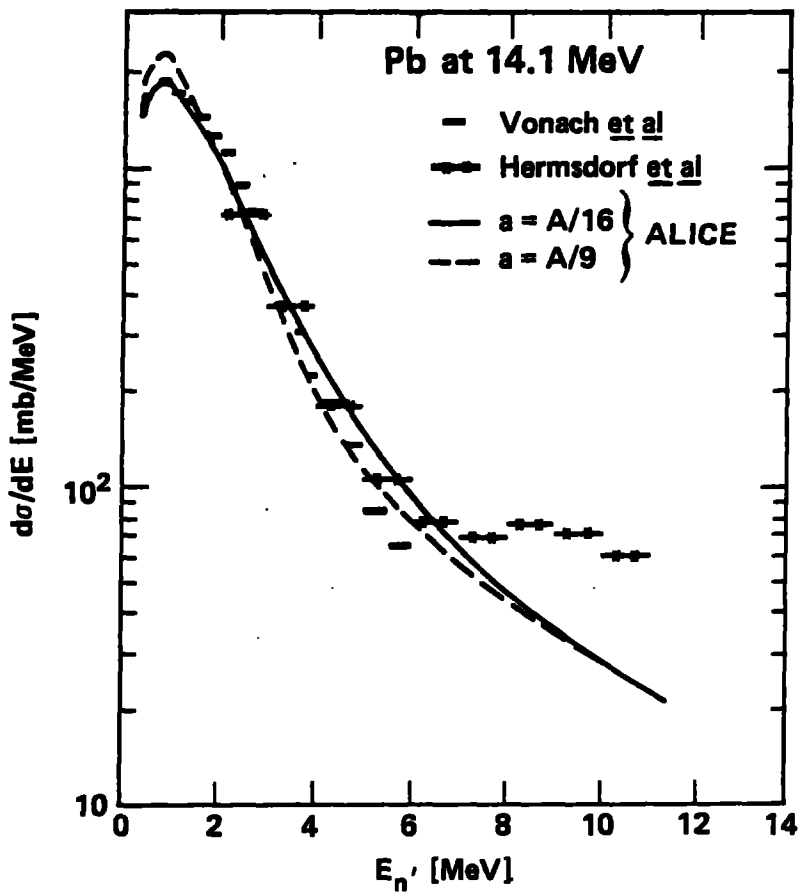
Pb at 14.1 MeV
Vonach et al
Hermsdorf et al
a = A/16
a = A/9
ALICE
dσ/dE [mb/MeV]
10²
10
0
2
4
6
8
10
12
14
E_n' [MeV]

Fig. 11